Electronic Supplementary Information

for

High Aspect Ratio WO_3 Nanostructures Anodically Grown in a Hot Pure o-H_3PO_4 Electrolyte and their use as H_2 Gas-sensors

by Marco Altomare,[1] Ole Pfoch,[1] Alexei Tighineanu,[1] Robin Kirchgeorg,[1] Kiyoung Lee,[1] Elena Selli[2] and Patrik Schmuki[1,3]*

[1] Department of Material Science and Engineering, WW4-LKO, University of Erlangen-Nuremberg, Martensstrasse 7, D-91058 Erlangen, Germany

[2] Department of Chemistry, University of Milan, Via C. Golgi 19, I-20133 Milan, Italy

[3] Department of Chemistry, King Abdulaziz University, Jeddah, Saudi Arabia

C O N T E N T S

Growth of anodic WO_3 layers on non-conductive glass

W layers (600-700 nm-thick, see Fig. S1) were deposited by e-beam evaporation (PLS 500 Labor System, Balzers-Peiffer, Germany) on non-conductive glass substrates at a pressure of 1-6 x 10^{-6} mbar and with a deposition rate of 0.1 nm s^{-1}. Tungsten granules (2-4 mm, 99.9 %, Chempur) were used as source of metal. Prior to the evaporation, the glass substrates (7.5 cm x 2.5 cm microscope glass slides, VWR) were cut into 1.2 cm x 2.5 cm pieces, degreased by ultrasonication (in acetone, ethanol and DI H_2O for 10 min each) and finally dried in a N_2 stream.

The W films on non-conductive glass were all anodized in optimized conditions, that is, in hot pure o-H_3PO_4 at 5 V and 100°C (see below for optimization of the anodization parameters). The anodization experiments were carried out in a two-electrode electrochemical cell where the W film and Pt gauze were the working and the counter electrodes, respectively. The two electrodes were immersed into the electrolyte in vertical configuration and placed at a distance of 2 cm from each other. The electrolyte was constantly stirred and kept at the desired temperature by thermostatic control provided by a heating-stirring plate. The heating plate was equipped with a thermocouple that was fully wrapped in Teflon tape and immersed into the anodizing electrolyte. The experiments were performed in potentiostatic conditions, that is, by applying a constant direct current potential of 5 V (no sweeping) provided by a Volcraft VLP 2403 Pro power source. The current density was recorded by using a Keithley 2100 6 ½ Digit multimeter interfaced with a laptop.

The anodization experiments were run long enough to anodize through the entire thickness of the W layer, *i.e.*, not to have a metallic W layer left beneath the anodic film (Fig. S1). For this, the current density was online monitored so that anodization experiments could be stopped when the W film was fully anodized, that is, when the current density significantly dropped (see Fig. 1(g)-(i) in the main text).

By anodizing for *ca*. 4 h in such experimental conditions, gas-sensors based on transparent porous WO_3 layers were formed that exhibited excellent adhesion to the glass slide. This configuration of the gas-sensors, *i.e.*, an anodic WO_3 films formed on non-conductive glass slide (see a sketch of the device in Scheme S1), was adopted because in preliminary experiments (WO_3 films on W foils or on FTO slides) we found the measurements to be strongly affected by the presence of a conductive substrate. In particular, the sensitivity of devices fabricated on conductive substrates was relatively low, this because the current flowed preferentially through the conductive substrate, and changes in resistance of the anodic film upon exposure to analytes became negligible compared to the overall resistance of the device. In other words, more reproducible results and higher sensitivity were obtained for gas-sensors fabricated from WO_3 films grown on non-conductive glass.

Growth of anodic WO_3 layers on W foil

Preliminary anodization experiments were carried out on W foils in order to optimize the experimental conditions, that is, to obtain high aspect ratio WO_3 films with vertically aligned nanochannels. The results of preliminary anodization experiments are summarized in Tables S1-S3 (see below).

For these experiments, W foils (0.125 mm thick, 99.95% purity, Advent Research Materials LTD, Oxford, UK) were cut into 1 cm x 2 cm pieces, cleaned by ultra-sonication in acetone, ethanol and de-ionized (DI) water (10 min each) and finally dried in a N_2 stream.

The anodization experiments were carried out in a two-electrode electrochemical cell, as reported above. The experiments were mainly performed in potentiostatic conditions, that is, by applying a constant direct current potential of 1-60 V (no sweeping) provided by a Volcraft VLP 2403 Pro power source. The current density was recorded by using a Keithley 2100 6 ½ Digit multimeter interfaced with a laptop. A galvanostatic experiment was also performed (Fig. S7). For this, the current density was set at 1.2 mA cm^{-2}. The resulting potential was recorded by using the same set-up described above.

The electrolyte was mainly composed of pure ortho-phosphoric acid (o-H_3PO_4, ≥ 99 %, Sigma-Aldrich). However, during the preliminary experiments, a few additives were also added to the electrolyte. Precisely, DI H_2O (18.2 MΩ cm), Ethylene Glycol (Fluka Analytical, ≥ 99.5 %) and Glycerol (Sigma Aldrich, ≥ 99.5 %) were used as additives for the o-H_3PO_4-based electrolytes.

Also pyrophosphoric acid ($H_4P_2O_7$, ≥ 90 %, Fluka Analytical) and polyphosphoric acid (115 %, Sigma-Aldrich) were used (as received, *i.e.*, pure).

Characterization of anodic WO_3 layers

A Hitachi FE-SEM S4800 was used for morphological characterization of the samples. The thickness of the anodic films was directly obtained from SEM cross-sectional micrographs. In the case of anodic WO_3 layers on W foils, the cross-sectional view was obtained by scratching off the anodic film with a blade. In the case of anodic WO_3 layers on non-conductive glass, the cross-sectional view was obtained either by scratching off the anodic film or by cracking the glass slides (for this, a diamond tip was used). EDAX (EDAX Genesis, fitted to SEM chamber) was also used for the chemical analysis.

Transmission electron microscopy (TEM) was performed by using a Philips CM300 UltraTWIN, equipped with a LaB6 filament and operated at 300 kV. TEM images and selective area diffraction (SAED) patterns were recorded with a fast scan (type F214) charge-coupled device camera from TVIPS (Tietz Video and Image Processing Systems), with an image size of 2048 x 2048 pixels. For TEM investigations, the samples were mechanically scratched from the substrate and the resulting powder was deposited on copper TEM grids coated with lacey carbon film.

XRD patterns were collected using an X'pert Philips PMD diffractometer with a Panalytical X'celerator detector, using graphite-monochromatized CuKα radiation (λ = 1.54056 Å).

Composition and chemical state of samples were determined by X-ray photoelectron spectroscopy using a PHI 5600 Multi-Technique System (Physical Electronics, USA) equipped with a monochromatic Al Kα X-ray source (1486.6 eV).

Fabrication of gas-sensors

As shown in Scheme S1, the fabrication of the gas-sensing devices was completed by annealing the porous WO_3 layers and by depositing Pt electrodes on their top. XRD analysis showed that as-formed anodic films are typically amorphous (Fig. 2(a)) and preliminary gas-sensing experiments revealed that crystallization of the oxide is a key to fabricate functional gas-sensors (Fig. 3(a)). Thus, the WO_3 films were annealled in air at different temperatures (250-650°C range) for 1 h, with a heating/cooling rate of 30°C min^{-1} by using a Rapid Thermal Annealer (Jipelec JetFirst100).

Then, the anodic films were contacted on top by depositing two 200 nm-thick Pt electrodes by using a Leica EM SCD 500 plasma sputtering system and applying a mask over the WO_3 films (Fig. S15). The deposition was carried out at 16 mA and at a rate of 0.16-0.20 nm s^{-1} (vacuum conditions, 10^{-2} mbar of Ar).

Gas-sensing experiments

For the gas-sensing measurements, the device was placed into the sensing chamber (Scheme S2) and flushing with artificial air (Linde, Germany) was carried out until reaching constant device resistance. The chamber was kept under thermostatic control by using a Eurotherm 3216-based temperature controller (Invensys Eurotherm, USA).

Gold wires were connected to the Pt electrodes that were sputter-deposited onto the annealed anodic WO_3 films. The resistance of the film was measured with a Keithley 2400 Source Meter (Keithley Instruments, USA) by applying a bias of 1 V. Preliminary experiments showed that the I-V characteristics of the WO_3 layers exhibited an ohmic response (not shown).

To investigate the device sensitivity, the WO_3 films were exposed to different concentration of H_2. For this purpose, different amounts of H_2-Ar mixtures (90.000 ppm of H_2 in Ar, Linde, Germany) were injected into the background stream of artificial air. The flow of the different gases was controlled with digital mass flow controllers MF1 (MKS Instruments, Germany). The relative response *r* of the sensors was calculated according to following equation:

$$r = \frac{R_0 - R}{R_0} \cdot 100\ \%$$

where R_0 and R are the resistance of the sensor when exposed to background air flow and to the H_2 injection, respectively.

Fig. S1 - (a,b) Top view and (c,d) cross-sectional SEM images of 600 nm-thick W film evaporated onto non-conductive glass slide; (e,f) Top view and (g,h) cross-sectional SEM images of 1.3 µm-thick WO_3 nanochannel layer formed by complete anodization of the 600 nm-thick W film in pure o-H_3PO_4 at 5 V and 100°C.

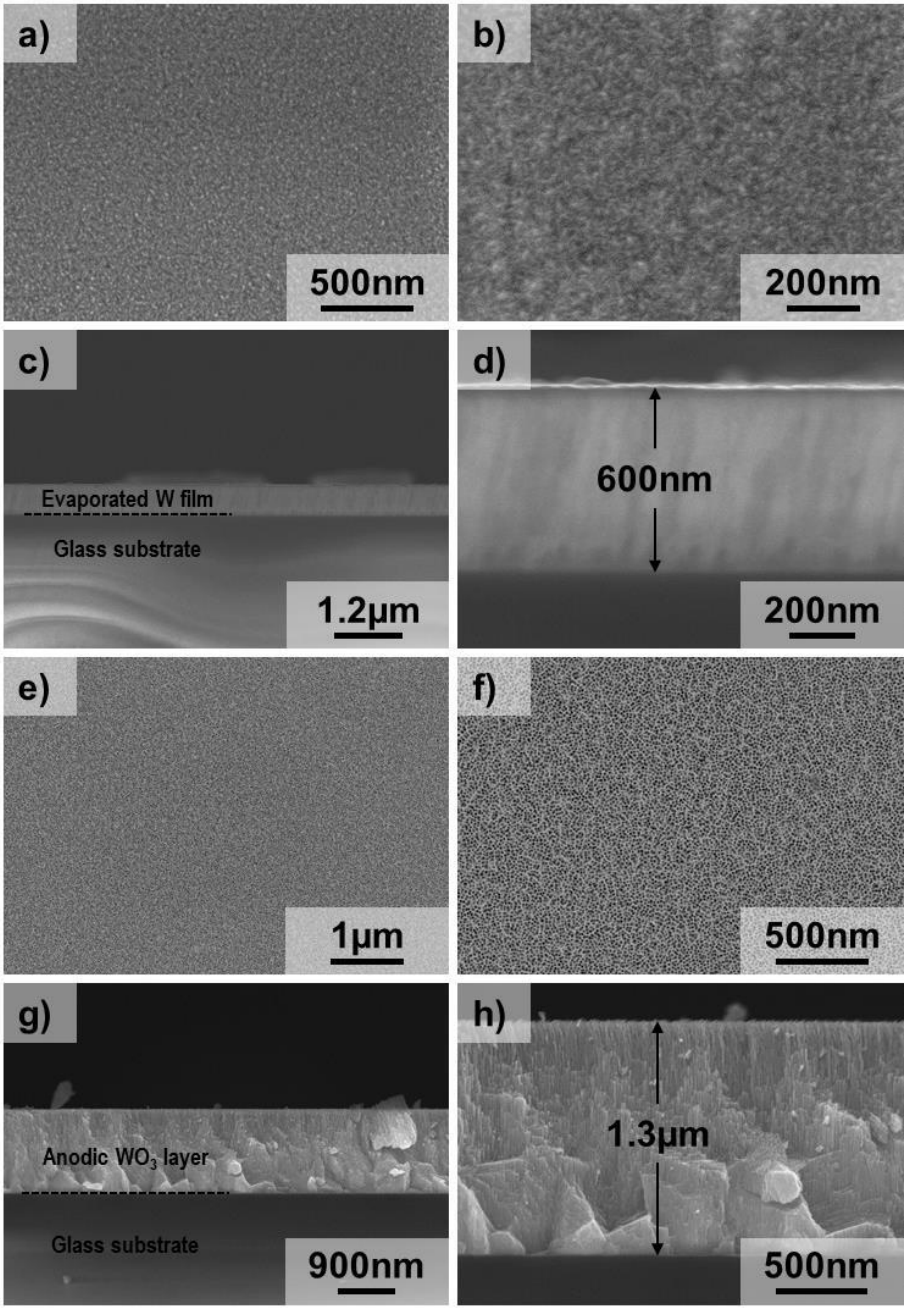

Fig. S2 - Analysis of the morphological features of the WO_3 nanochannel structures grown under optimized conditions (pure o-H_3PO_4, 5 V, 100°C). (a) Cross sectional SEM image and (b) relative gray profile plot (taken over the area in the red box and along the direction indicated by the arrow); (c) top view SEM image and (d) relative statistical distribution of pore size. Inset: Gaussian fitting of the experimental data shown in (d). The processing of SEM images was performed by using the software Image J.

The analysis of the morphological features of the anodic structures reveals that these layers are composed of a multitude of highly-aligned vertically-oriented WO_3 nanochannels with pore diameter in the *ca*. 10-20 nm. Precisely, Gaussian fitting (inset) of the experimental data shown in (d) reveals that the mean pore size is of 10 nm.

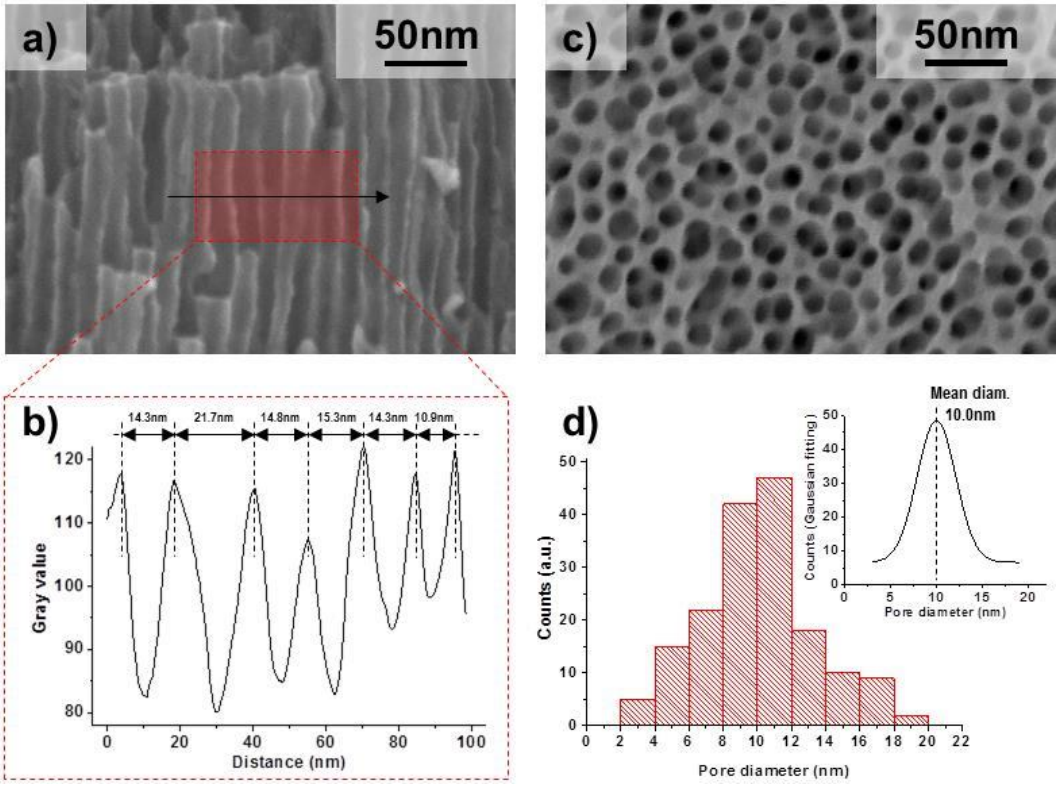

Table S1 - Anodization experiments carried out on W foils in pure molten o-H_3PO_4[§].

T (°C)	E (V)	TIME (h)	DESCRIPTION	THICKNESS
20	20	0.5	Little extent of etching	Not measured
	30			
	40		Large extent of etching	
20	5	1	Compact oxide layer	Few tens of nm
40				
60				
80			Porous layer	Few tens of nm
80	20	1	Channels with a little extent of etching at the top	400 – 500 nm
	40		Large extent of etching	Not measured
100	1	1	Porous layer	Few tens of nm
	2.5		Highly ordered nanochannels, smooth and flat at the top	300 nm
	5			300 – 400 nm
	5*			
	10			400 – 500 nm
	10	4		0.8 – 1.1 µm
	15	1	Nanochannels with a little extent of etching at the top	1.2 – 1.3 µm
	20		Porous layer	1.3 – 1.4 µm
100	5	0.5	Porous layer	150 – 200 nm
		2	Highly ordered nanochannels, smooth and flat at the top	600 – 700 nm
		4		1.3 – 1.5 µm
		8		1.9 – 2.1 µm
		12	Ordered nanochannels with nanograss[†] at the top	2.1 – 2.6 µm
		24		3.4 – 3.6 µm
	2.5	24		1.0 – 1.1 µm
120	5	1	Nanochannels with a little extent of etching at the top	400 – 500 nm
90	5	1	Highly ordered nanochannels, smooth and flat at the top	100 – 200 nm
95				200 nm
105				400 – 450 nm
110				1.0 – 1.1 µm
110[‡]				800 – 900 nm
115			Ordered nanochannels with grass at the top	1.0 – 1.3 µm

[§]o-H_3PO_4 = ortho-phosphoric acid; solid at room temperature (melting point = 42.3°C).

*the electrolyte was aged by anodizing a W foil for 100 h at 2.5 V and 100°C.

[‡]the electrolyte was aged by anodizing a W substrate for 25 h at 5V and 110°C.

[†]the term "nanograss" refers to needle-like nanosized structures that form at the top of the anodic layer because of a large extent of etching (typically observed for extended anodization experiments).

Table S2 - Anodization experiments carried out on W foils in o-H_3PO_4-based electrolytes.

ADDITIVE	T (°C)	E (V)	TIME (h)	DESCRIPTION	THICKNESS
H_2O traces*	110	5	1	Ordered nanochannels with grass at the top	1.0 – 1.1 µm
0.5vol.%H_2O	100			Highly ordered nanochannels, smooth and flat at the top	300 – 400 nm
1vol.%H_2O	20	5	0.5	Compact oxide layer	Not measured
		20			
		40		Little extent of etching	
2vol.%H_2O	100	5	1	Highly ordered nanochannels, smooth and flat at the top	500 – 600 nm
		10			
		15		Channels with a little extent of etching at the top	
5vol.%H_2O	20	5	0.5	Compact oxide layer	Not measured
		20			
		40		Little extent of etching	
		60		Electropolishing	
10vol.%H_2O	20	5	0.5	Compact oxide layer	Not measured
		20			
		40		Large extent of etching	
	100	5	1	Ordered nanochannels with grass at the top	0.9 – 1.1 µm
		10	0.5		0.6 – 1.1 µm
25vol.%EG‡	100	5	1	Highly ordered nanochannels, smooth and flat at the top	300 – 400 nm
		20	0.3	Large extent of etching	Not measured
25vol.%GLY†	50	10	1	Compact oxide layer	Not measured
		20			
	80			Porous layer	Few tens of nm
	100	10	0.3	Ordered nanochannels, smooth and flat at the top	300 – 400 nm

*the electrolyte was exposed overnight to ambient air to allow for moisture uptake and no preliminary heat treatment was performed before anodizing.

‡EG = Ethylene glycol.

†GLY = Glycerol.

Table S3 - Anodization experiments carried out on W foils in other hot pure phosphorus-containing acid electrolytes.

ACID	T (°C)	E (V)	TIME (h)	DESCRIPTION	THICKNESS
$H_4P_2O_7$*	100	5	1	Porous layer	Few tens of nm
		20		Channels with a large extent of etching	250 – 300 nm
		40	0.3	Large extent of etching	Not measured
	110	5	1	Highly ordered nanochannels, smooth and flat at the top	1.0 – 1.1 µm
		10			
		20		Channels with a large extent of etching	450 – 550 nm
	120	5		Highly ordered nanochannels, smooth and flat at the top	1.1 – 1.2 µm
POLY‡	120	5	1	Ordered nanochannels, smooth and flat at the top	200 – 250 nm

*$H_4P_2O_7$ = pyrophosphoric acid; solid at room temperature (melting point = 71.5°C).
‡POLY = polyphosphoric acid; viscous liquid at room temperature.

Fig. S3 - (a,b) Top view and (c,d) cross sectional SEM images of 0.64 µm-thick ordered WO_3 nanochannel layer grown by anodizing a W foil for 2 h, in pure o-H_3PO_4 at 5 V and 100°C.

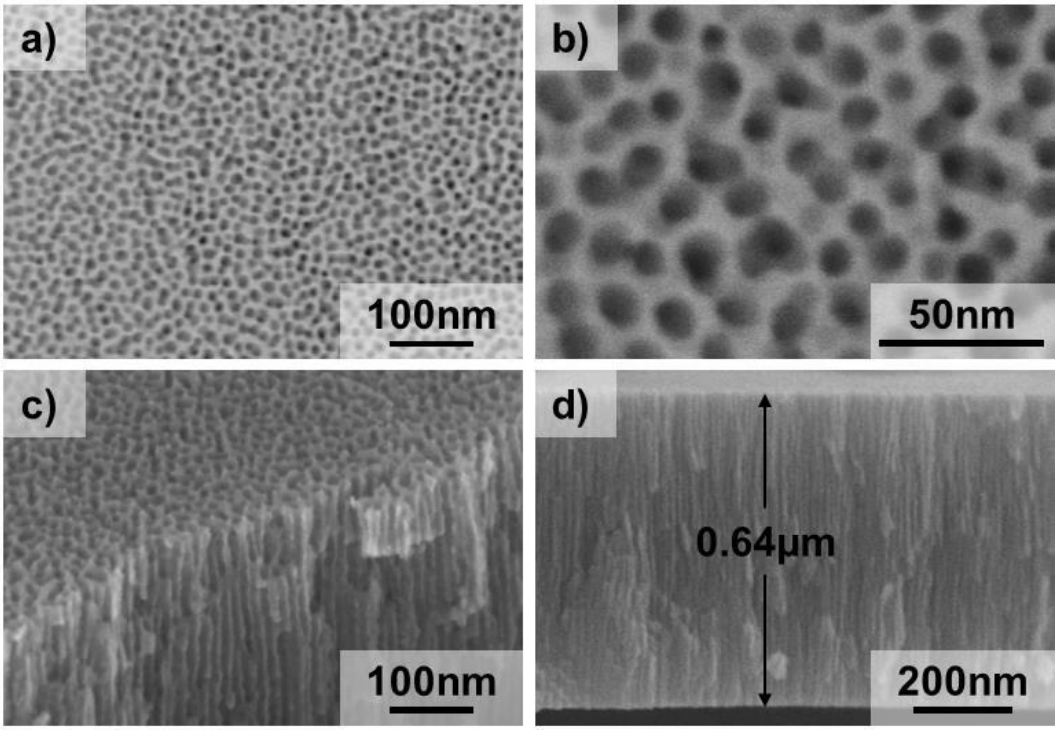

Fig. S4 - SEM images of anodic WO_3 films grown on W foils in pure o-H_3PO_4 at 5 V for 1 h, with temperature of the electrolyte of (a) 60, (b) 80 and (c) 120°C. The scale bars are of 100 nm. In the case of the anodic layer in (b), no clear cross sectional image could be taken (*i.e.*, a few nm-thick film).

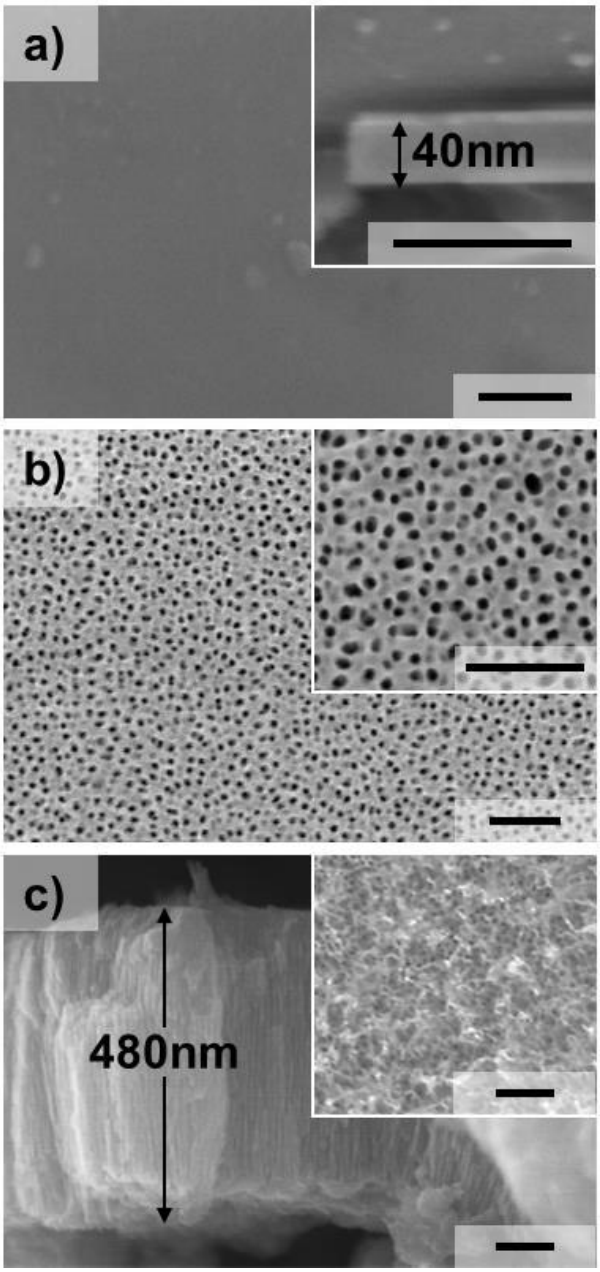

Fig. S5 - Current density (J) *vs*. time profiles of anodization experiments carried out on W foils in pure o-H_3PO_4 at 100°C for 1 h, at different applied potential in the 1-20 V range. The plot in the red box shows a magnified view of the J-time profiles of experiments carried out at 1, 2.5, 5 and 10 V.

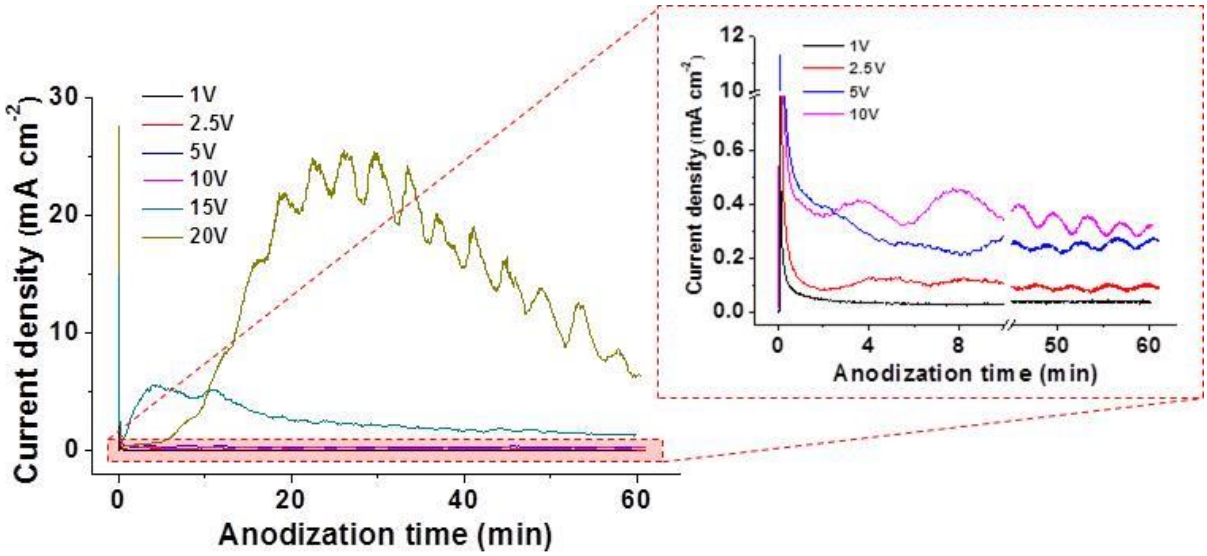

Fig. S6 - Top view and (insets) cross sectional SEM images of WO_3 layers fabricated by anodization of W foils in pure o-H_3PO_4 at 100°C for 1 h, at applied potential of (a) 1, (b) 2.5, (c) 5, (d) 10, (e) 15 and (f) 20 V. The relative J-time profiles are shown in Fig. S5. The scale bars are of 100 nm, aside from when otherwise specified.

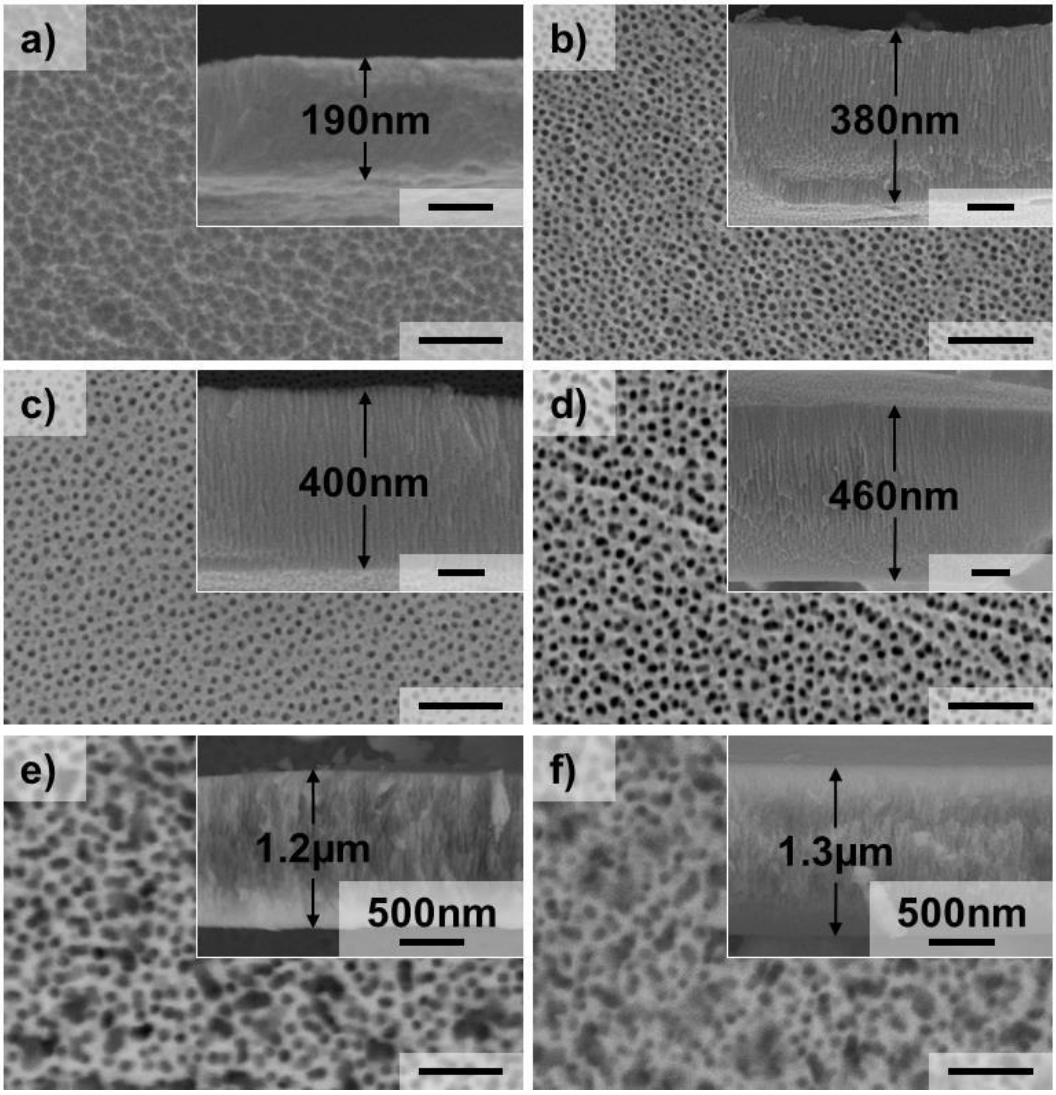

Fig. S7 - (a) Potential *vs*. time profile recorded for galvanostatic (J of *ca*. 1.2 mA cm^{-2}) anodization of W foil in pure o-H_3PO_4 at 100°C for 1 h; (b) cross sectional and (c,d) top view SEM images of the anodic layer grown in galvanostatic condition.

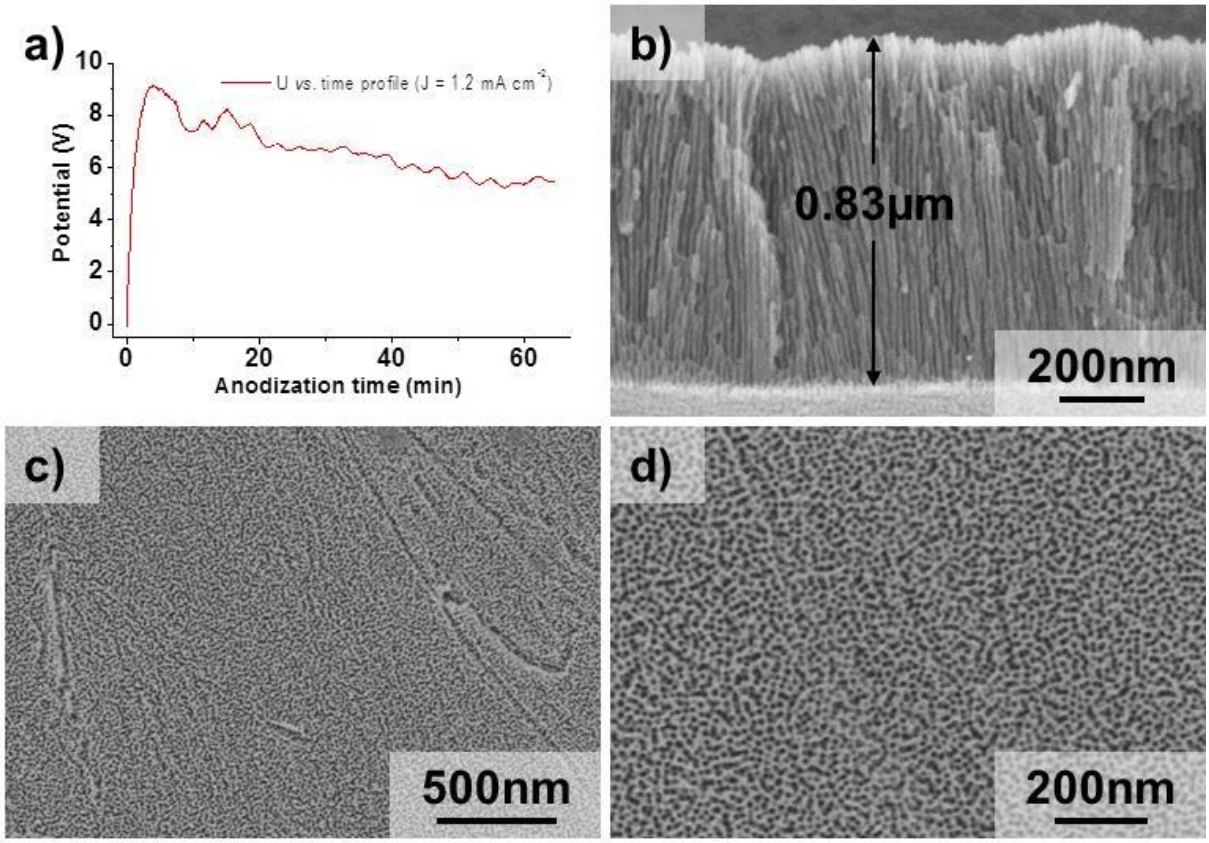

Fig. S8 - (a) J-time profile of an anodization experiment performed on W foil in optimized conditions (pure o-H_3PO_4 at 5 V and 100°C) during which, after *ca*. 30 min of anodization, 100 µL of DI H_2O were added to the hot o-H_3PO_4 electrolyte (so to reach a DI H_2O concentration of *ca*. 0.5 vol%). The inset shows a magnified view of the J-time profile; (b) top view SEM image of the anodic film grown as reported in (a); (c-f) top view and cross sectional (insets) SEM images of anodic WO_3 films grown at 5 V and 100°C in o-H_3PO_4-based electrolytes with initial water contents of (c,d) 2 and (e,f) 10 vol%.

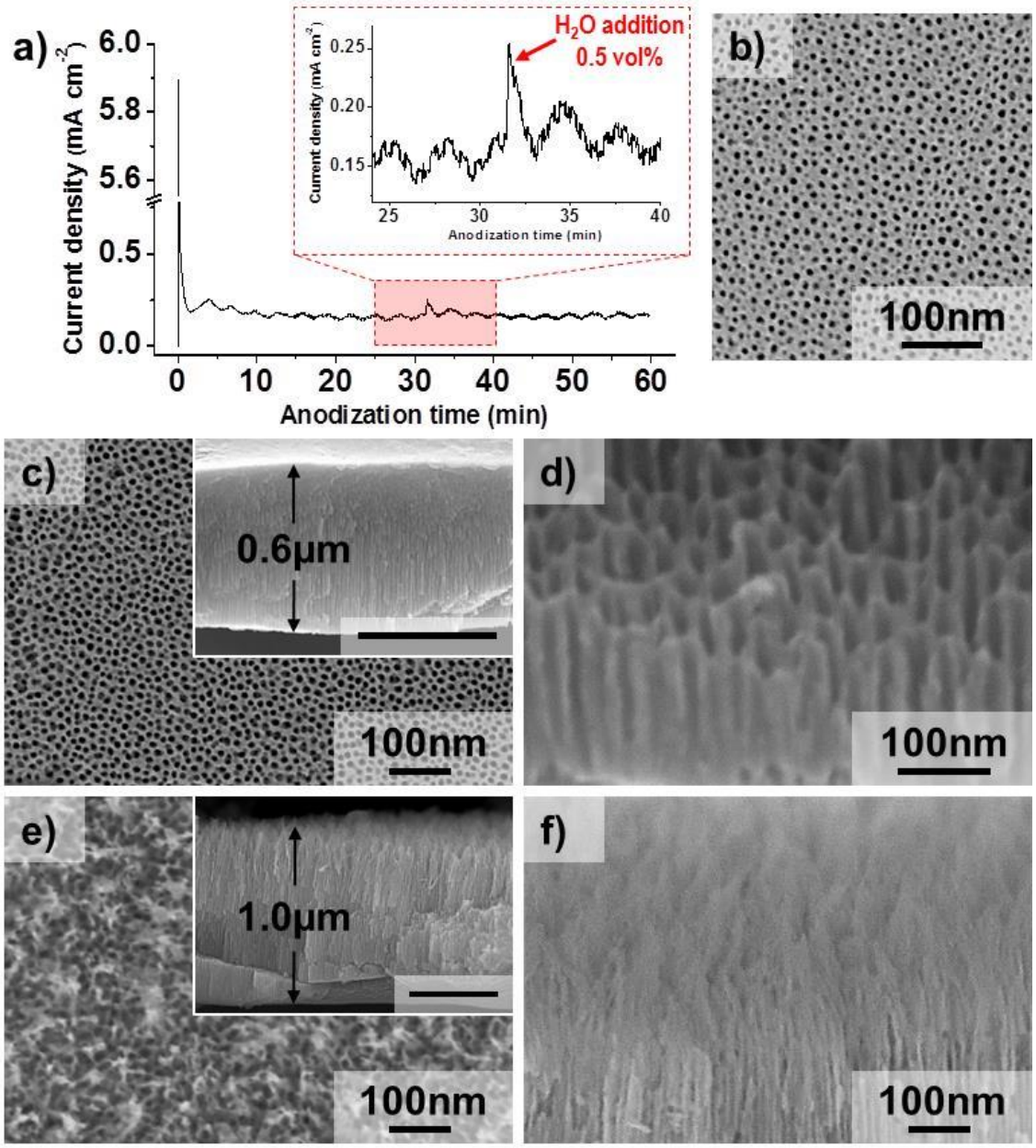

Fig. S9 - a) Oxide layer thickness *vs*. anodization time for WO_3 nanochannels grown on W foil under optimized conditions (pure o-H_3PO_4 at 5 V and 100°C). The plot in the red box shows the linear correlation between layer thickness and anodization time for 0.5-8 h-long experiments; (b-g) top view and cross sectional SEM images of WO_3 nanochannel layers grown by anodizing W foils for (b,c) 4 and (d-g) 24 h in optimized conditions (pure o-H_3PO_4 at 5 V and 100°C).

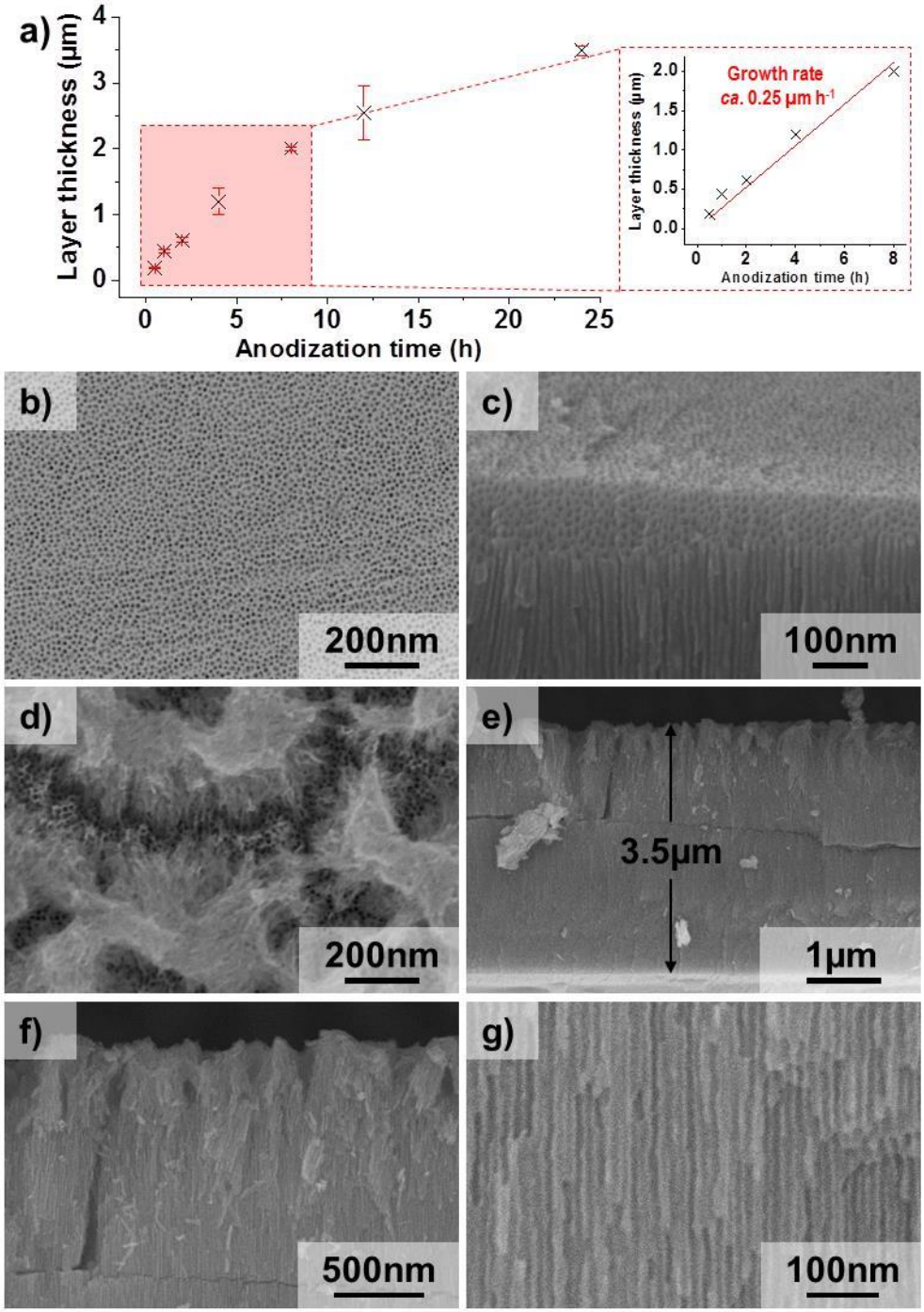

Fig. S10 - (a,c) Top view and (b,d) cross sectional SEM images of WO_3 nanochannel layers grown by anodizing W foils at 120°C (5 V, 1 h) in pure (a,b) pyro- and (c,d) poly-phosphoric acid.

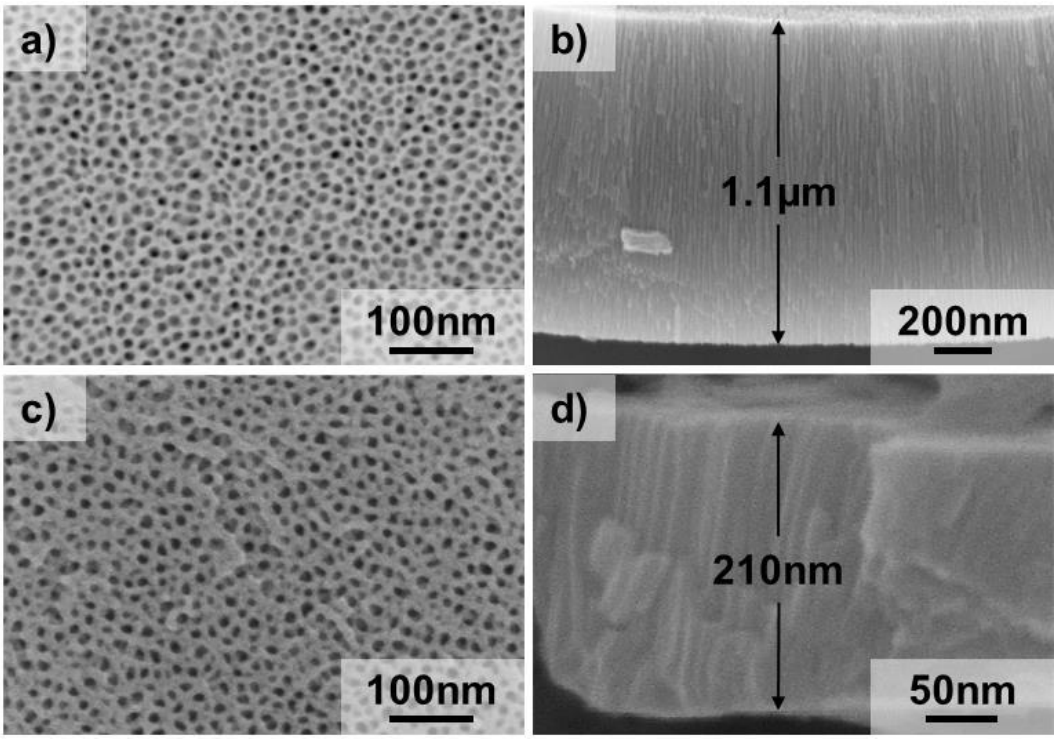

Fig. S11 - (a,b) Top view and (c,d) cross sectional SEM images of aluminum oxide nanopores grown by anodizing for 1h Al foils in pure o-H_3PO_4 at 40 V and room temperature.

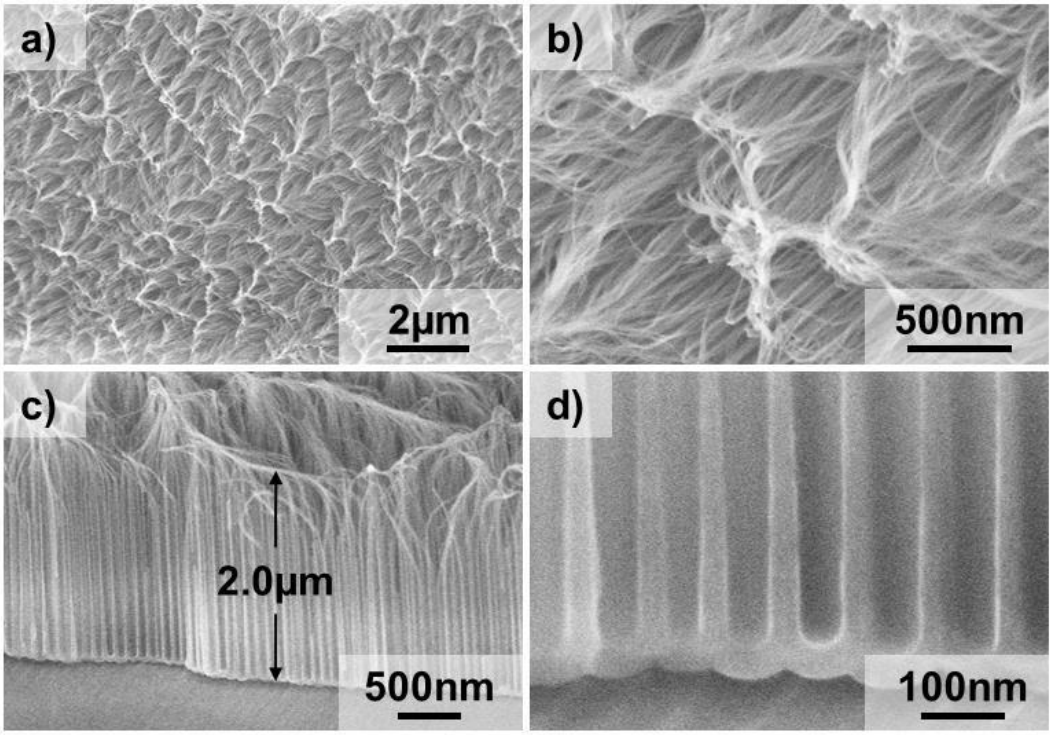

Fig. S12 - (a,b) Top view and (c,d) cross sectional SEM images of niobium oxide nanochannels grown by anodizing for (a,b) 1 h and (c,d) 12 h Nb foils in pure o-H_3PO_4 at 10 V and 100°C.

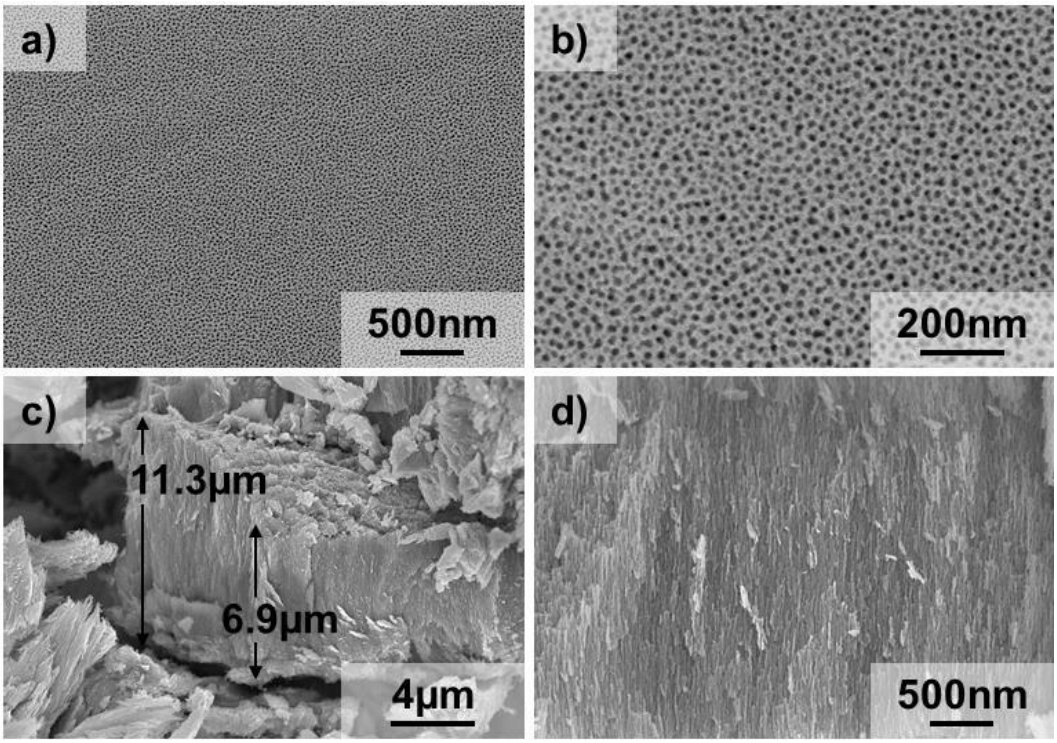

Scheme S1 - (a) Sketch of the different steps for fabricating the gas-sensors (see above for details on crystallization of the anodic layer and deposition of the Pt electrodes); (b) sketch of resistive gas-sensor configuration adopted in this work, that is, with the anodic nanoporous WO_3 film grown on non-conductive glass; (c) sketch of an alternative configuration for resistive gas-sensor that implies the direct growth of the anodic layer on the metal foil or, more generally, on a conductive substrate.

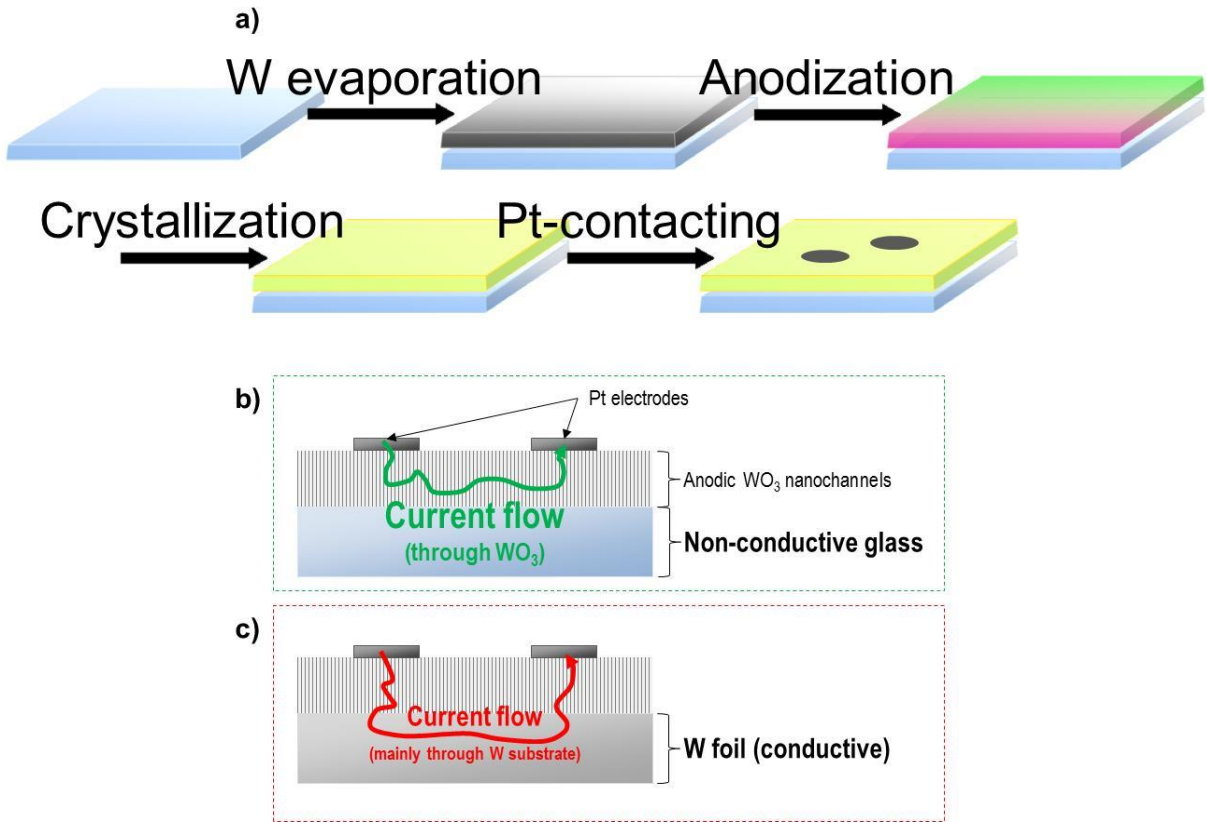

Fig. S13 - SEM images of gas-sensing devices fabricated from WO_3 nanochannel layers that were anodically grown in optimized conditions on non-conductive substrate and annealed at (a,b) 450, (c-e) 550 and (f) 650°C (air, 1 h).

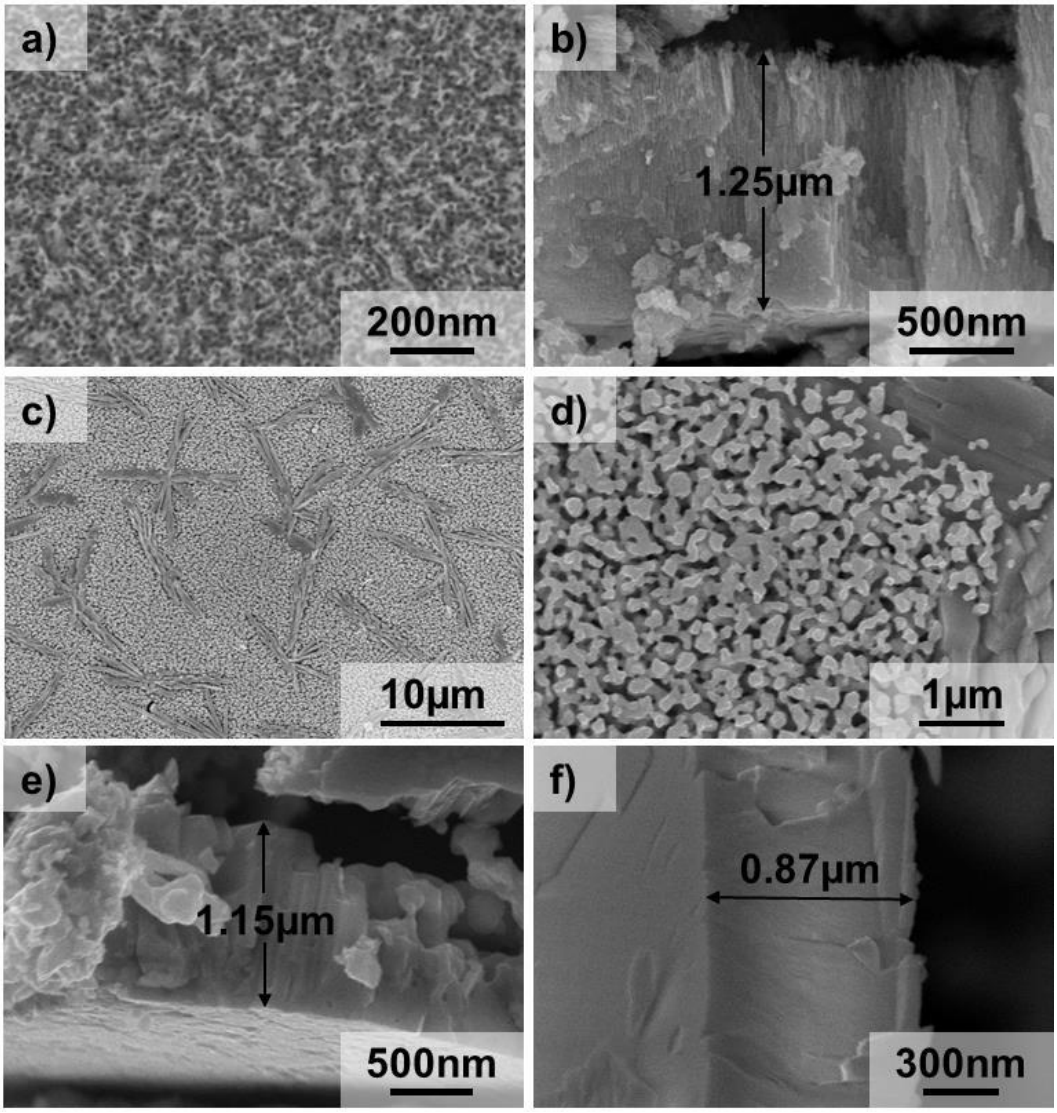

Fig. S14 - (a,c) EDAX spectra and (b,d) relative data of (a,b) as-formed and (c,d) annealed (450°C) WO_3 nanochannel layers that were anodically grown on W foils in optimized conditions. The peak of Aluminum (detected for both as-formed and annealed films) is ascribed to the aluminum sample holder.

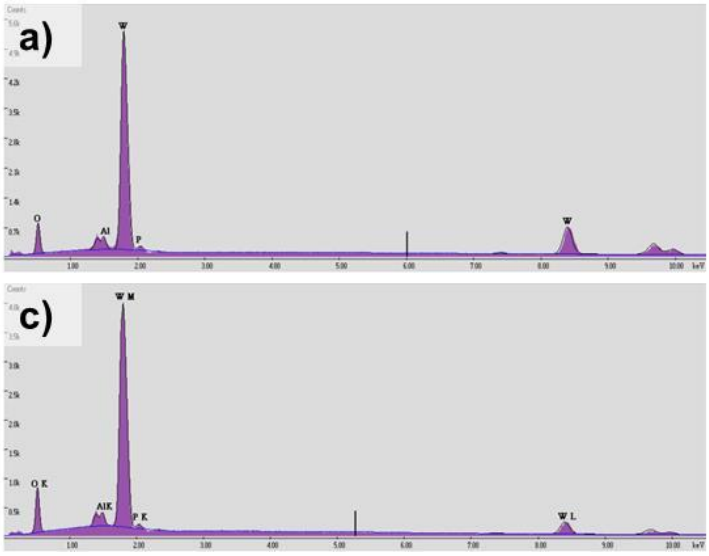

b)

Element	Wt%	At%
O K	14.95	63.70
Al K	1.80	4.56
PK	0.48	1.07
WL	82.76	30.68

d)

Element	Wt%	At%
O K	13.21	60.94
Al K	1.40	3.83
PK	0.49	1.17
WL	84.90	34.07

Scheme S2 - Sketch of the gas-sensing setup.

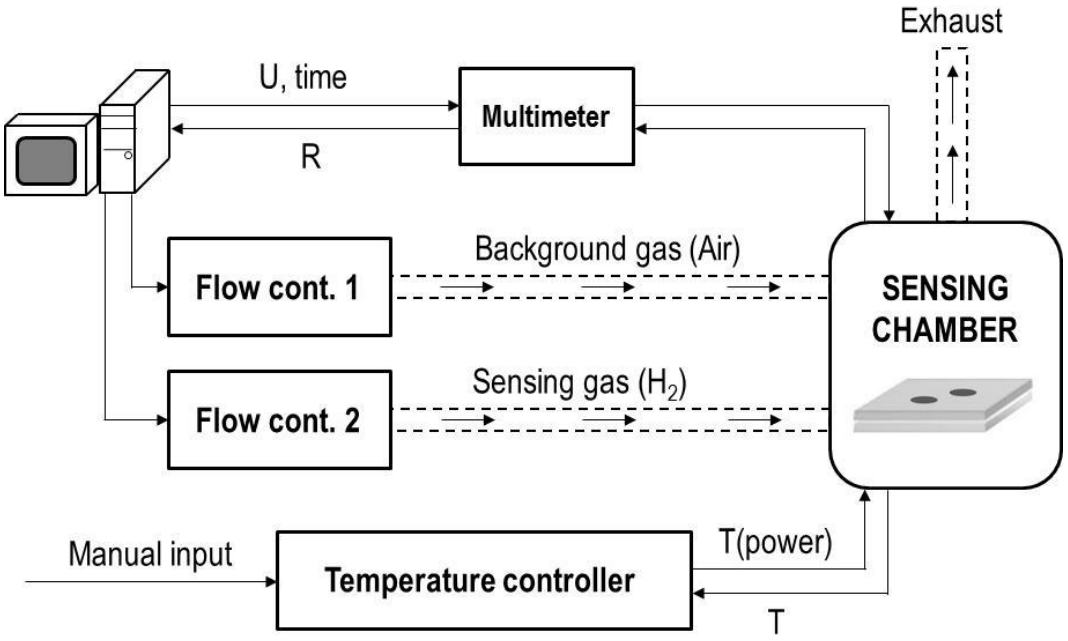

Fig. S15 - (a) Optical and (b,c) top view SEM images of a gas-sensing device fabricated from WO_3 nanochannel layers that were anodically grown in optimized conditions on non-conductive glass substrates; (b) low magnification top-view SEM image of the device showing the anodic layer and the two sputtered Pt electrodes; (c) high magnification top-view SEM image of the sputtered Pt electrode.